



# The Structure of a Transient Complex of a Nonribosomal Peptide Synthetase and a Cytochrome P450 Monooxygenase\*\*

Kristina Haslinger, Clara Brieke, Stefanie Uhlmann, Lina Sieverling, Roderich D. Süssmuth, and Max J. Cryle\*

**Abstract:** Studying the interplay between nonribosomal peptide synthetases (NRPS), a major source of secondary metabolites, and crucial external modifying enzymes is a challenging task since the interactions involved are often transient in nature. By applying a range of synthetic inhibitor-type compounds, a stabilized complex appropriate for structural analysis was generated for such a tailoring enzyme and an NRPS domain. The complex studied comprises an NRPS peptidyl carrier protein (PCP) domain bound to the Cytochrome P450 enzyme that is crucial for the provision of  $\beta$ -hydroxylated amino acid precursors in the biosynthesis of the cyclic depsipeptide skyllamycin. The structure reveals that complex formation is governed by hydrophobic interactions, the presence of which can be controlled through minor alterations in PCP structure that enable selectivity amongst multiple highly similar PCP domains.

Nonribosomal peptide synthesis is responsible for the production of important secondary metabolites such as penicillin,<sup>[1]</sup> cephalosporin,<sup>[1]</sup> and vancomycin.<sup>[2]</sup> Given the modular organization of nonribosomal peptide synthetases (NRPS) and their interplay with multiple amino acid modifying and decorating enzymes, expansion of the biological toolbox far beyond the limits of ribosomal biosynthesis is possible.<sup>[3]</sup> This makes the investigation of NRPS and their interaction partners of great interest for both basic research and biotechnological applications.<sup>[2]</sup> The majority of the

amino acid precursors required for NRPS biosynthesis are synthesized prior to selection by the NRPS.<sup>[4]</sup> However, a new paradigm for precursor production through the selective, direct interaction of modifying proteins and NRPS-bound amino acids has recently been demonstrated for the cyclic depsipeptide skyllamycin.<sup>[5,6]</sup> This process involves the  $\beta$ -hydroxylation of hydrophobic amino acids bound to carrier protein (CP) domains by a Cytochrome P450 (P450) enzyme (Figure 1).<sup>[7,8]</sup> The selection mechanism involved is dependent

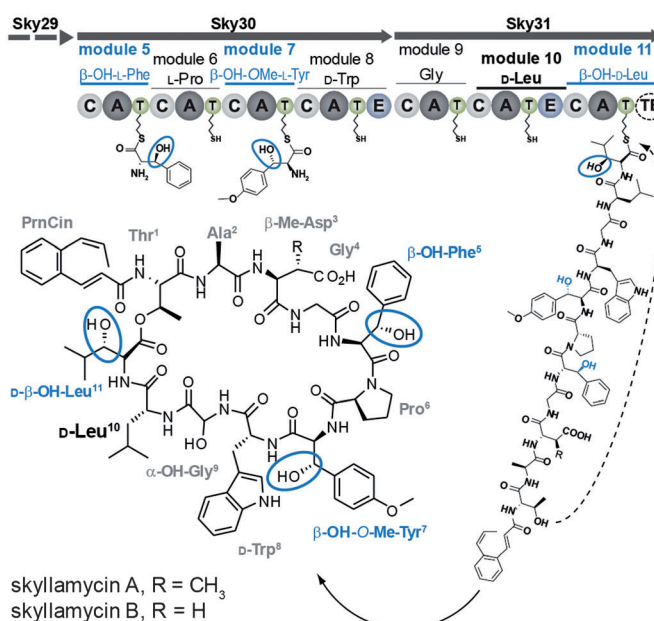


**Figure 1.** A schematic overview of skyllamycin biosynthesis in which only the relevant modules are shown (Sky29, Sky30, and Sky31). C: condensation, A: adenylation, E: epimerisation, T: peptidyl carrier protein or thiolation domain.

not upon the amino acid residues themselves but rather the respective CP domains<sup>[9]</sup> and clearly offers great potential for exploitation in the modification of nonribosomal peptides in vivo.

To understand the basis of P450/CP selectivity in this system, it was essential to structurally characterize the complex, since isolated P450 structures offer limited clues to the origins of the selectivity.<sup>[7,10]</sup> Structural analysis was complicated by the weak interaction between the proteins involved, which precluded co-crystallization. To overcome this difficulty, we exploited the fact that the ferric heme group of P450s coordinates nitrogen ligands in a highly stable, inhibitor-like manner.<sup>[11]</sup> We synthesized an array of inhibitors

[\*] K. Haslinger, Dr. C. Brieke, L. Sieverling, Dr. M. J. Cryle  
Department of Biomolecular Mechanisms  
Max Planck Institute for Medical Research  
Jahnstrasse 29, 69120 Heidelberg (Germany)  
E-mail: Max.Cryle@mpimf-heidelberg.mpg.de  
Dr. S. Uhlmann, Prof. Dr. R. D. Süssmuth  
Institut für Chemie, Technische Universität Berlin  
Strasse des 17. Juni 124, 10623 Berlin (Germany)

[\*\*] We thank A. Koch and E. Maximowitsch (MPI-Hd) for assistance with protein expression and the collection of binding spectra; A. Meinhardt and T. Barends (MPI-Hd) for assistance with data processing; J. Yin (University of Chicago) for the R4-4 Sfp expression plasmid; G. Stier (BZH-Hd) for the thioredoxin fusion-protein vector; and C. Roome (MPI-Hd) for IT support. Diffraction data were collected at the Swiss Light Source, X10SA beamline, Paul Scherrer Institute, Villigen, Switzerland. We thank the Heidelberg team for data collection and the PXII staff for their support in setting up the beamline. M.J.C. is grateful for the support of the Deutsche Forschungsgemeinschaft (Emmy-Noether Program, CR 392/1-1), R.D.S. to the Cluster of Excellence (UniCat) of the DFG and for DFG-Project: SU 239/12-1.

Supporting information for this article is available on the WWW under <http://dx.doi.org/10.1002/anie.201404977>.

linked to coenzyme A, loaded them onto the isolated peptidyl carrier protein (PCP) domains *in vitro*, and used these as “bait” to trap the P450/PCP complexes. This approach allowed us to crystallize the complex formed between the P450 and PCP<sub>7</sub> from skylamycin biosynthesis, thereby revealing that whilst the secondary structure elements forming the CP interface are similar to those of other NRPS-CP complexes,<sup>[12]</sup> these exist in a novel arrangement within the P450/PCP complex. Furthermore, the origins of PCP selectivity cannot be found in the primary sequence of the directly interacting residues; rather the selectivity appears to originate from minor alterations to the relative arrangement of the helices of different PCPs, thus limiting the generation of competent binding interfaces to specific PCPs that interact with the P450.

Studying the interaction of NRPS carrier domains with partners that act in *trans* is challenging. Firstly, PCPs removed from their multidomain surroundings are often unstable, aggregation-prone, or unable to be modified by transferases. Secondly, moderate affinity and the transient character of the interactions further complicate experiments. In this study we utilized two PCPs from the skylamycin NRPS: the P450-interacting PCP<sub>7</sub> and the non-interacting PCP<sub>10</sub>, both fused to a thioredoxin tag.<sup>[13]</sup> In analogy to previous studies on carrier protein interactions,<sup>[12,14,15]</sup> we were able to show that decreasing the dissociation of the P450/PCP complex through the use of special inhibitor-like carrier protein cargos is a valuable technique for trapping NRPS CP/P450 complexes. To design the probe, we exploited the long-lived and stable interaction of heterocyclic nitrogen coordination to Fe<sup>III</sup>,<sup>[11]</sup> as exemplified by imidazole (**1**, Figure 2, and Figure S2 and Table S2 in the Supporting Information). We designed an array of inhibitor-like binding probes as three different

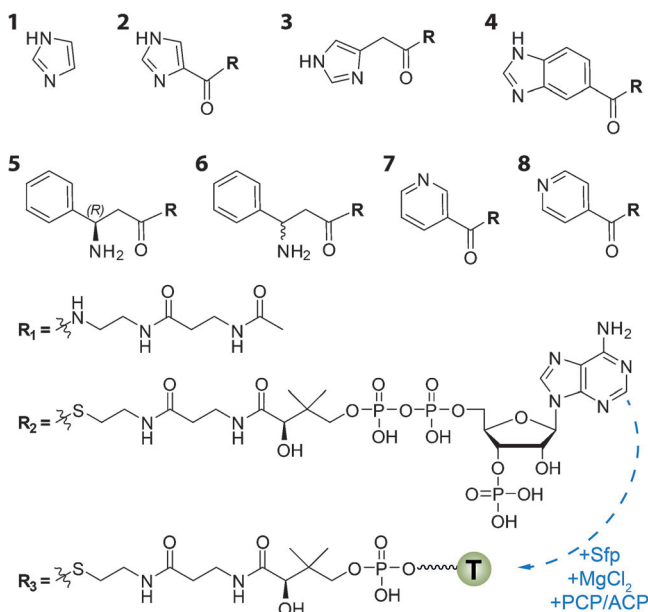


**Figure 2.** An overview of the inhibitors applied in this study (**1**–**8**) as three different conjugates: **R**<sub>1</sub> = shortened pantetheine amide, **R**<sub>2</sub> = CoA thioester and **R**<sub>3</sub> = thioester of 4'-phosphopantetheinylated carrier proteins (PCP<sub>7</sub>, PCP<sub>10</sub>, or ACP).

conjugates: a shortened amide of pantetheine (**R**<sub>1</sub>), a coenzyme A thioester (CoA, **R**<sub>2</sub>), and the CoA thioester loaded onto carrier proteins (**R**<sub>3</sub>: PCP<sub>7</sub>, PCP<sub>10</sub>, or ACP; Figure 2, Supporting Information Figure S1, Table S1). The inhibitors were based on imidazole derivatives (**2**, **3**) and other types of nitrogen-containing and/or heterocyclic inhibitors (**4**–**8**). This series of probes provides a range of distances between the CP and the heme-coordinating nitrogen atom, as well as alternate degrees of rotational freedom and substrate mimicry. We investigated the binding behavior of these PCP conjugates by UV/Vis spectroscopy in order to choose the best ones for crystallization; controls were performed with imidazole (**1**), its **R**<sub>1</sub> and **R**<sub>2</sub> conjugates (**2**–**R**<sub>1</sub>–**R**<sub>2</sub>), and ACP- or PCP<sub>10</sub>-loaded **2**–**R**<sub>3</sub>. As expected, titration of the P450 from the skylamycin synthesis pathway (P450<sub>sky</sub>) with imidazole leads to a typical type-II (N coordination, inhibitor-type) spectral shift with a *K*<sub>d</sub> of 2.6 ± 0.2 mM (see the Supporting Information).

Titration with conjugate **2**–**R**<sub>2</sub> evokes a substrate-like type-I shift (Figure S2b), as reported.<sup>[7,10]</sup> The binding spectra for **2**–**R**<sub>1</sub> display an anti-type-II shift (Figure S2b), which corresponds to hydrogen bonding between heme-bound water and the ligand nitrogen atom.<sup>[16]</sup> Based on how P450<sub>sky</sub> accepts hydrophobic cargo from interacting PCP domains,<sup>[7]</sup> we then presented our PCP<sub>7</sub> conjugates to the P450 (Figure 3). As

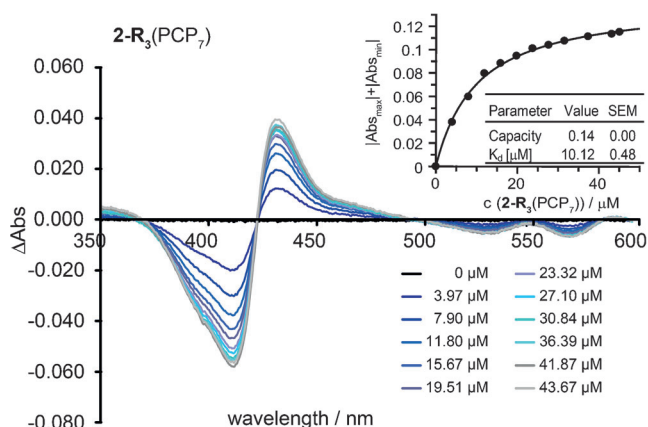


**Figure 3.** UV/Vis difference spectra of P450<sub>sky</sub> titrated with **2**–**R**<sub>3</sub>(PCP<sub>7</sub>). Extrapolated amplitudes were plotted against the titrant concentration and fitted to a one-site binding model (inset).

anticipated, **2**–**R**<sub>3</sub>(PCP<sub>7</sub>) binds in a manner similar to **1** but with a dissociation constant two orders of magnitude smaller (*K*<sub>d</sub> = 10.1 ± 0.5 μM), and that is binding tighter than the natural substrate (OMe)-Tyr (*K*<sub>d</sub> = 89 ± 3 μM).<sup>[7]</sup> The non-interacting PCP<sub>10</sub> and *E. coli* ACP were loaded to form **2**–**R**<sub>3</sub>(PCP<sub>10</sub>/ACP), and these conjugates showed no significant binding or spectral shift (Figure S2e,f). We thus conclude that the observed binding of **2**–**R**<sub>3</sub>(PCP<sub>7</sub>) is highly specific and occurs under the influence of two driving forces: protein–protein interaction and the coordination of the inhibitor nitrogen to ferric heme.

Compounds **3**–**8**–**R**<sub>3</sub>(PCP<sub>7</sub>) were examined for binding to P450<sub>sky</sub>. Strong and highly reproducible inhibitor-type spectral shifts were obtained with **3**–, **4**–, and **6**–**R**<sub>3</sub>(PCP<sub>7</sub>), whereas the

other compounds proved less effective (Table S2 and Figure S3). Co-crystallization experiments were then undertaken using compounds (**2-4-R<sub>3</sub>** and **6-R<sub>3</sub>**) and we were able to crystallize the P450<sub>sky</sub>/2-R<sub>3</sub>(PCP<sub>7</sub>) protein complex for which all previous attempts without the use of tethered inhibitors had failed.

Phases were initially obtained from a single anomalous dispersion experiment with selenomethionine labeled crystals (3.0 Å resolution), with a native data set then refined to 2.7 Å (Table S3). P450<sub>sky</sub> in the complex adopts the typical P450 fold (Figure 4)<sup>[11]</sup> with the only differences to the unbound P450<sub>sky</sub> structure in the interface-forming F- and G-helices (RMSD Cα 1.7 Å; see Figure S4a,b).<sup>[7]</sup> There is a surprising lack of rearrangement of the B/B<sub>2</sub> or B<sub>2</sub>/C loops, which is

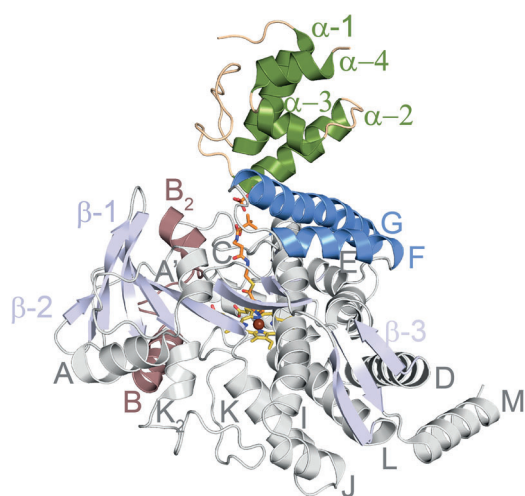


**Figure 4.** The complex of P450<sub>sky</sub> and PCP<sub>7</sub> trapped by an azole inhibitor. P450 is shown in grey, the interface-forming helices F and G in blue, the B/C region in red,  $\beta$ -sheets in light blue, and heme in yellow. PCP is depicted in gold and green and the inhibitor is shown in orange. All secondary structure features are labeled.

generally observed in substrate-bound P450 structures.<sup>[11]</sup> PCP<sub>7</sub> adopts the expected fold of a four-helix bundle with two major ( $\alpha$ -1,  $\alpha$ -2) and two minor ( $\alpha$ -3,  $\alpha$ -4) helices. The conserved serine residue (S42) that bears the posttranslational modification (4'-phosphopantetheine derived from coenzyme A) is located at the beginning of  $\alpha$ -2. The well-ordered PCP<sub>7</sub> peptide chain starts several residues after the start of the PCP<sub>7</sub> sequence<sup>[\*]</sup>, with no density present for thioredoxin. PCP<sub>7</sub> is structurally related to several ACP<sup>[17]</sup> and PCP<sup>[9,14]</sup> structures (Table S5), including ACP from the P450<sub>Biol</sub>/ACP complex (RMSD Cα 1.6 Å, Figure S5).<sup>[17]</sup> Structural alignment with P450<sub>sky</sub> identified P450<sub>Biol</sub>,<sup>[17]</sup> OxyD,<sup>[10]</sup> and various mycobacterial P450s as the structures of highest structural similarity (Table S4). The P450<sub>sky</sub>/PCP<sub>7</sub> interface contains few ionic interactions or hydrogen bonds: R63 ( $\alpha$ -3), T46 ( $\alpha$ -2), and K47 ( $\alpha$ -2) of PCP<sub>7</sub> contact D191 (G-helix), N197 (G-helix), and E235 (I-helix) of the P450, respectively (Figure 5a), whilst the amino group of L62 in  $\alpha$ -3 forms a water-mediated hydrogen bond with E198. In contrast, the hydrophobic character of the interface is more pronounced: in both protein folds, clusters of hydrophobic residues can be identified that accommodate a hydrophobic residue of the interaction partner. W193 and L194 of the P450 (Figure 5b) are in close proximity (4–5.6 Å) to residues forming a hydrophobic pocket within the PCP<sub>7</sub> helix bundle, and L43 of PCP<sub>7</sub> reaches into a smaller cleft between the I- and G-helix and the C/D loop of the P450 (residues shown in blue, 4–5.5 Å). This hydrophobic pocket also accommodates the *gem*-dimethyl groups of the pantetheine linker. The interface is thus dominated by hydrophobic interactions between secondary structure elements. Similar interface architectures with hydrophobic character have been observed in the structures of carrier proteins in complex with domains of NRPS<sup>[14,15,18]</sup> or amino acid ligases.<sup>[19]</sup> Complementary to

[\*] Residue 6, corresponding to residue 3079 of Sky30 in UniProt numbering.

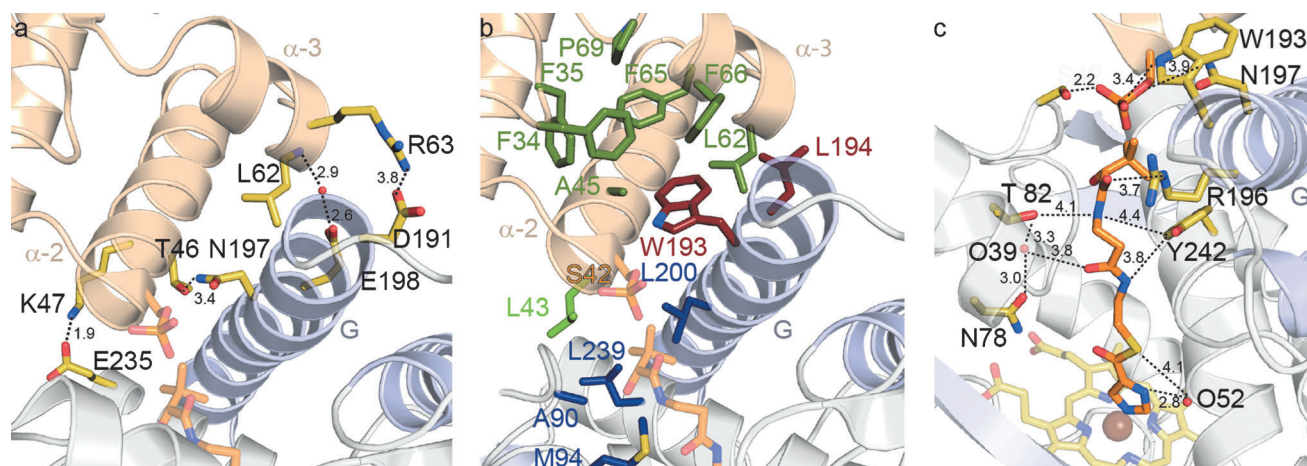


**Figure 5.** The protein–protein interface (a,b) and active site (c) of the P450<sub>sky</sub>/PCP<sub>7</sub> complex. P450<sub>sky</sub> is shown in blue-grey and PCP<sub>7</sub> in gold. a) Hydrogen bonds (black dotted lines) are formed across the interface. b) Hydrophobic pockets are formed on both protein surfaces. The residues shown in blue form a pocket on the P450 side to accommodate L43 of PCP<sub>7</sub> (light green) and the two methyl groups of Ppant (orange). The PCP<sub>7</sub> residues shown in green form a large cavity to accommodate W193 and L194 of P450<sub>sky</sub> (red). c) Hydrogen bonds (dotted lines) are formed between the residues lining the substrate entry channel of the P450 (yellow) and the Ppant linker carrying the azole inhibitor (orange).



the protein–protein interactions, several residues lining the P450 substrate entry channel are in close proximity to the Ppant cofactor, however, the distances allow weak hydrogen bonding interactions at best (Figure 5c). Such an arrangement may stem from the inhibitor-Ppant moiety, which is fixed on either end by the S42–Ppant and Fe–N bonds (set to 2.0 Å during refinement and justified by the electron density, see Figure S6). This inhibitor thus cannot rotate freely around the bond between the carboxy and imidazole groups. The other strongly interacting inhibitor conjugates [3-, 4- and 6- $\mathbf{R}_3$ (PCP<sub>7</sub>)], which do not possessing such strain, failed to crystallize, most likely owing to additional rotational and conformational freedom.

The interface residues identified in the P450<sub>sky</sub>/PCP<sub>7</sub> complex are highly conserved amongst all carrier proteins of the skylamycin NRPS. Additionally, there is no major rearrangement of the P450 upon complex formation—indeed all amino acid oxidizing P450s appear to maintain their structure through interactions provided by a defined consensus sequence<sup>[10]</sup>—and thus proper arrangement of the interface-forming surfaces is required prior to contact of the proteins. This observation implies that alterations to the PCP tertiary structure are the most likely explanation for selectivity. Comparison of a model of the non-interacting PCP<sub>10</sub> with that of the binding-competent PCP<sub>7</sub> in complex with P450<sub>sky</sub> shows that such differences manifest themselves in minor changes to the orientations of helices  $\alpha$ -2 and  $\alpha$ -3 (Figure S7), which result in alterations to and probable loss of the hydrophobic interaction site involving W193/L194 of P450<sub>sky</sub>.

With regards to PCP/P450 orientation, the positioning of PCP<sub>7</sub> relative to P450<sub>sky</sub> is very different from the only related complex, that of P450<sub>Biol</sub>/ACP.<sup>[17]</sup> PCP<sub>7</sub> occupies the space above the P450<sub>sky</sub> G-helix so that  $\alpha$ -2 is present at a 25° angle to the heme plane and projects from the center of the P450 to the periphery (Figure 4). Helices  $\alpha$ -2 and  $\alpha$ -3 form an X-shaped cleft that accommodates the G-helix (5a,b). The Ppant linker carrying the azole protrudes from S42 at a similar angle with respect to the heme plane as the bound fatty acids in the P450<sub>Biol</sub>/ACP complex, albeit from a very different entry site (Figure 6). In the P450<sub>Biol</sub>/ACP structure, ACP  $\alpha$ -2 is centered between the F/G-loop and the B/B<sub>2</sub>-loop of the P450 and projects along the cleft between the  $\alpha$ -helical half and the  $\beta$ -strand-rich half of the P450. The ACP Ppant and cargo enter the P450<sub>Biol</sub> active site from the  $\beta$ -strand-rich half close to the  $\beta_2$ -turn, approach the heme, and then project upwards towards the F-helix. Apart from the P450<sub>sky</sub> M-helix, the structures of the P450s are highly congruent (RMSD Ca 2.2 Å). Minor differences are seen in the F- and G-helices and major differences in the region between the B/C helices (Table S6 and Figure S8). This area strongly influences the binding mode of the carrier protein. Substrate-free structures of related NRPS/PKS interacting P450s are compatible with the P450<sub>sky</sub>/PCP<sub>7</sub> (OxyD)<sup>[10]</sup> and P450<sub>Biol</sub>/ACP (CalO2)<sup>[20]</sup> complex binding modes (PKS = Polyketide synthases). The characterization of further P450/CP complexes, for example, those involved in the biosynthesis of macrolide<sup>[21]</sup> or glycopeptide antibiotics,<sup>[22]</sup> will establish whether the binding modes now described are exhaustive for PKS- and NRPS-type complexes.

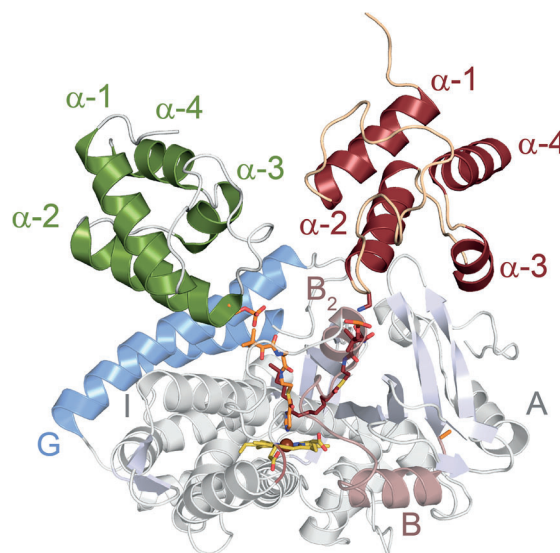


**Figure 6.** Superposition of P450<sub>sky</sub>/PCP<sub>7</sub> with P450<sub>Biol</sub>/ACP based on the P450 polypeptide chains. Only ACP, P450<sub>sky</sub> and PCP<sub>7</sub> are shown (ACP and tetradecanoic acid are shown in red, P450<sub>sky</sub> and PCP<sub>7</sub> are colored as in Figure 4).

In summary, we present an approach that enabled the first structural characterization of a transient P450/PCP interaction. Given the importance of such interactions in non-ribosomal peptide synthesis, and their potential role in polyketide synthesis systems, we anticipate that our strategy for isolating P450/CP complexes, as well as the structure of P450<sub>sky</sub>/PCP<sub>7</sub> itself and its implications, will prove an important platform for future investigation and the eventual alteration of the selectivity of such NRPS-interacting modifying enzymes in vivo.

Received: May 5, 2014

Published online: July 9, 2014

**Keywords:** bioorganic chemistry · biosynthesis · metalloenzymes · protein–protein interactions · structural biology

- [1] J. E. Baldwin, E. Abraham, *Nat. Prod. Rep.* **1988**, *5*, 129–145.
- [2] K. M. G. O'Connell, J. T. Hodgkinson, H. F. Sore, M. Welch, G. P. C. Salmond, D. R. Spring, *Angew. Chem.* **2013**, *125*, 10904–10932; *Angew. Chem. Int. Ed.* **2013**, *52*, 10706–10733.
- [3] M. A. Fischbach, C. T. Walsh, *Chem. Rev.* **2006**, *106*, 3468–3496.
- [4] G. H. Hur, C. R. Vickery, M. D. Burkart, *Nat. Prod. Rep.* **2012**, *29*, 1074–1098.
- [5] S. Pohle, C. Appelt, M. Roux, H.-P. Fiedler, R. D. Süßmuth, *J. Am. Chem. Soc.* **2011**, *133*, 6194–6205.
- [6] V. Schubert, F. Di Meo, P.-L. Saaïdi, S. Bartoschek, H.-P. Fiedler, P. Trouillas, R. D. Süßmuth, *Chem. Eur. J.* **2014**, *20*, 4948–4955.
- [7] S. Uhlmann, R. D. Süßmuth, M. J. Cryle, *ACS Chem. Biol.* **2013**, *8*, 2586–2596.
- [8] M. J. Cryle, C. Brieke, K. Haslinger, *Oxidative Transformations of Amino Acids and Peptides Catalysed by Cytochromes P450*, Vol. 39 (Eds.: E. Farkas, M. Ryadnov), The Royal Society of Chemistry, London, **2014**, pp. 1–36.

- [9] T. Weber, R. Baumgartner, C. Renner, M. A. Marahiel, T. A. Holak, *Structure* **2000**, 8, 407–418.
- [10] M. J. Cryle, A. Meinhart, I. Schlichting, *J. Biol. Chem.* **2010**, 285, 24562–24574.
- [11] *Cytochrome P450. Structure, Mechanism and Biochemistry* (Ed.: P. R. Ortiz de Montellano), Kluwer Academics/Plenum, New York, **2005**.
- [12] J. Crosby, M. P. Crump, *Nat. Prod. Rep.* **2012**, 29, 1111–1137.
- [13] J. Bogomolovas, B. Simon, M. Sattler, G. Stier, *Protein Expression Purif.* **2009**, 64, 16–23.
- [14] Y. Liu, T. Zheng, S. D. Bruner, *Chem. Biol.* **2011**, 18, 1482–1488.
- [15] J. A. Sundlov, C. Shi, D. J. Wilson, C. C. Aldrich, A. M. Gulick, *Chem. Biol.* **2012**, 19, 188–198.
- [16] N. Mast, W. Zheng, C. D. Stout, I. A. Pikuleva, *J. Biol. Chem.* **2013**, 288, 4613–4624.
- [17] M. J. Cryle, I. Schlichting, *Proc. Natl. Acad. Sci. USA* **2008**, 105, 15696–15701.
- [18] A. Tanovic, S. A. Samel, L.-O. Essen, M. A. Marahiel, *Science* **2008**, 321, 659–663.
- [19] M. Mocibob, N. Ivic, M. Luic, I. Weygand-Durasevic, *Structure* **2013**, 21, 614–626.
- [20] J. G. McCoy, H. D. Johnson, S. Singh, C. A. Bingman, I.-K. Lei, J. S. Thorson, G. N. Phillips, Jr., *Proteins* **2009**, 74, 50–60.
- [21] L. Song, L. Laureti, C. Corre, P. Leblond, B. Aigle, G. L. Challis, *J. Antibiot.* **2014**, 67, 71–76.
- [22] D. Bischoff, S. Pelzer, B. Bister, G. J. Nicholson, S. Stockert, M. Schirle, W. Wohlleben, G. Jung, R. D. Süßmuth, *Angew. Chem.* **2001**, 113, 4824–4827; *Angew. Chem. Int. Ed.* **2001**, 40, 4688–4691.